Interactions of warming and altered nutrient load timing on the phenology of oxygen dynamics in Chesapeake Bay

Nicole Basenback, Jeremy M. Testa, and Chunqi Shen

College of Agriculture and Natural Resources (Basenback), University of Maryland, College Park, Maryland, USA; and Chesapeake Biological Laboratory (Testa), University of Maryland Center for Environmental Science, Solomons, Maryland, USA; and College of Biological and Environmental Sciences (Shen), Nanjing Forestry University, Nanjing, Jiangsu, China (Correspondence to Testa: jtesta@umces.edu).

Keywords: eutrophication < ECOLOGY, total maximum daily loading (TMDL) < WATER QUALITY, estuaries < GEOGRAPHY, Chesapeake Bay, climate variability/change < CLIMATE, Metabolism, biogeochemical model

Research Impact Statement: Climate change impacts on agriculture, watershed processes, and estuarine biogeochemistry interact to potentially drive a seasonal shift in the consumption of oxygen and associated hypoxia.

ABSTRACT: The effects of nutrient loading on estuaries are well-studied, given the multitude of negative water quality and ecosystem effects that have been attributed to excess nitrogen and phosphorus. A current gap in this knowledge involves the sensitivity of seasonal cycles of estuarine biogeochemical processes to direct (warming) and indirect influences (nutrient load timing) of climate change. We used a coupled hydrologic-biogeochemical model to investigate changes in the phenology of hypoxia and related biogeochemical processes in Chesapeake Bay under three different hydrologic regimes. Shifts to earlier nutrient load timing during idealized simulations reduced the overall annual hypoxic volume, resulting from discernable, but relatively small reductions in phytoplankton biomass and both sediment and water-column respiration. Simulated increases in water temperature caused an increase in spring/early summer hypoxic volume associated with elevated respiration rates, but an associated exhaustion of organic matter in the early summer caused a decrease in late summer/fall hypoxic volume due to lowered respiration. Warming effects on hypoxia were larger than nutrient timing effects in scenarios where warming was restricted to spring and when it was applied to all months of the year. These idealized simulations begin the process of understanding the potential impacts of future climatic changes in the seasonal timing of key biogeochemical processes associated with eutrophication.

Introduction

The impacts of nutrient loading on estuaries have been well-studied over the past several decades (Boynton, Kemp, & Keefe, 1982; Riemann et al., 2015; Scavia, Justic, & V.J. Bierman, 2004), due to the multitude of negative water quality, ecosystem, and economic impacts that have been attributed to excess nitrogen and phosphorus concentrations. The extent and duration of low dissolved oxygen waters are increasing in frequency and scale worldwide (Breitburg et al., 2018), in part because high rates of microbial respiration result from elevated phytoplankton production, fueled by these excess nutrients, and consume oxygen (Chen, Gong, & Shiah, 2007; Kemp, Sampou, & Boynton, 1987). Low dissolved oxygen conditions impart physiological stress on many mobile and sessile aquatic organisms and can influence behavior (Brady, Targett, & Tuzzolino, 2009; Breitburg, 1994; Díaz & Rosenberg, 1995), motivating many large-scale, expensive socio-economic commitments to reduce the extent and duration of hypoxia. Although modest reductions in nutrient loads have occurred in Chesapeake Bay and other estuaries worldwide (Kubo, Hashihama, Kanda, Horimoto-Miyazaki, & Ishimaru, 2019; Murphy, Kemp, & Ball, 2011; Riemann et al., 2015), many hypoxic volumes remain stable or are increasing (Turner, Rabalais, & Justic, 2008; Wang, Hu, Li, Yu, & Huang, 2018)

Climate change is expected to alter precipitation and temperature patterns that are expected to influence hypoxia via changes in nutrient inputs, metabolic rates, stratification ad oxygen solubility (Irby, Friedrichs, Da, & Hinson, 2018; Laurent, Fennel, Ko, & Lehrter, 2018; Meier et al., 2011; Ni, Li, Ross, & Najjar, 2019). Chesapeake Bay is expected to have larger hypoxic volumes in the future associated with climate change, given that contemporary warming has already compensated for expected improvements from nutrient loading (Ni, Li, & Testa, 2020) and that warmer temperatures are expected to reduced oxygen concentrations through

many pathways (Irby et al., 2018; Ni et al., 2019; Testa et al., 2021). Climate change impacts on precipitation will also influence hypoxia, as interannual variations in river flow are a key driver of hypoxia through stratification enhancement and elevated nutrient inputs (Hagy, Boynton, Keefe, & Wood, 2004; Li et al., 2016). Restoration efforts to reduce nutrient loads are expected to interact with these climate-induced changes in hypoxia.

Climate change also has the potential to alter myriad watershed processes. Agricultural activities that influence nutrient inputs (irrigation and fertilization) and water and soil temperatures that impact crop uptake and nutrient transformations in soils are sensitive to temperature and precipitation changes (Wagena et al., 2018). For example warmer spring temperatures have allowed for agricultural activities across much of the Midwest and Mid-Atlantic regions to begin earlier in recent years, where for example, corn planting occurs 6 days earlier from 1996-2012 compared to 1979-1995 in Pennsylvania (U.S. Department of Agriculture, 2010). Given that the agriculture sector has been identified as a considerable source of nutrient pollution to the Chesapeake Bay estuary (Boesch, Brinsfield, & Magnien, 2001), alterations to agricultural nutrient loads will have a significant effect on land-water nutrients fluxes. Fluctuations in climate can also mediate the seasonality in nutrient inputs because periods of high precipitation, when following several years of dry conditions, have the potential to flush high loads of dissolved nitrogen into the estuary (M. Lee, Shevliakova, Malyshev, Milly, & Jaffé, 2016). In forested parts of the Chesapeake Bay watershed, climate change has been linked to reduced nitrogen availability associated with earlier leaf-out during spring in temperate forests (Elmore, Nelson, & Craine, 2016), which will likely alter the timing and magnitude of nutrient export. Despite widespread evidence for seasonal changes to watershed processes, there remains

123 a limited understanding of how these potential seasonal changes to nutrient loading will impact
124 eutrophication and hypoxia in Chesapeake Bay.

125 While the impacts of climate variability on eutrophication and hypoxia have been well
126 studied, most prior analyses have focused on annual-scale ecosystem changes. However, many
127 key biogeochemical processes associated with oxygen have distinct annual cycles, and may be
128 characterized as having a phenology (Testa, Murphy, Brady, & Kemp, 2018). For example, the
129 timing of hypoxia initiation correlates strongly with winter-spring freshwater flow and the
130 associated accumulation of chlorophyll-*a* in bottom water (Y. J. Lee, Boynton, Li, & Li, 2013;
131 Testa & Kemp, 2014), both of which are strongly seasonally dependent. Testa et al. (2018)
132 observed a shift in hypoxic volume phenology between the time periods 1985-1999 and 2000-
133 2015, with the latter years experiencing a lower peak volume and slightly earlier cycle that
134 corresponded to a pattern of warming and a muted spring bloom. Examples in other estuaries
135 have suggested phenological changes in estuarine biogeochemistry associated with climatic
136 change, altering metabolism rates and the timing and magnitude of plankton production (Jahan &
137 Choi, 2014; Nixon et al., 2009; Stæhr, Testa, & Carstensen, 2017). Given the complexity of
138 relevant processes driving phenology and the subtle changes in timing (e.g., days) associated
139 with phenological shifts, there is a clear need to use tools with high spatial and temporal
140 frequency to understand long-term changes to seasonal timing.

141 Thus, the purpose of this paper was use a numerical modeling framework to understand
142 the potential changes in Chesapeake Bay hypoxia associated with altered seasonal timing of
143 nutrient inputs and increased water temperature. The Chesapeake Bay estuary is an ideal study
144 system for such an analysis given its strong response to external forces, characteristic seasonal
145 cycles, and hypoxia vulnerability to future climate. We used idealized numerical model

simulations to understand how changes in the seasonal timing of nutrient inputs and elevated water temperatures affect the seasonality and spatial response of hypoxia in the Chesapeake Bay.

Methods

To quantify the biogeochemical response of Chesapeake Bay hypoxia to altered timing of nutrient inputs and temperature, we conducted several idealized sensitivity simulations using a coupled, three dimensional hydrodynamic-biogeochemical model (ROMS-RCA). Model scenarios included changes in the timing of riverine nutrient concentrations that attempt to reflect expected changes in farmer behavior and watershed processes resulting from climate change, as well as seasonally-specific and annual-scale increases in water temperature that are consistent with observed temperature increases over the past 30 years. We investigated the seasonal biogeochemical response to altered external forcing by examining the volume of hypoxic water in the mainstem of Chesapeake Bay, chlorophyll-*a* accumulation during spring, and the associated respiratory processes in the water-column and sediments.

Numerical Model: A coupled hydrodynamic-biogeochemical model (Regional Ocean Modeling System and Row-Column Aesop, ROMS-RCA) was used to simulate and analyze estuarine biogeochemical responses to simulated changes in temperature and nutrient input timing. The application of ROMS has been validated against a wide range of observational data (Li, Zhong, & Boicourt, 2005; Li, Zhong, Boicourt, Zhang, & Zhang, 2007) and this application used a 80×120 grid points in the horizontal direction (about ~1 km grid size) and 20 layers in the vertical dimension (Fig. 1) as reported previously (Li et al., 2016). Freshwater inputs for ROMS-RCA are based on gauged inputs measured at the eight major Bay tributaries: including the Susquehanna, Patuxent, Patapsco, Potomac, Choptank, Rappahannock, York, and James Rivers.

169 Further details of the ROMS configuration are reported elsewhere (Li et al., 2016; Testa et al.,
170 2014). ROMS-generated salinity, water temperature, advective, and diffusive transport fields are
171 passed to the biogeochemical model (RCA) offline (i.e., soft coupling). RCA (Row-column
172 Aesop) is a biogeochemical model that simulates water column and sediment (aerobic and
173 anaerobic layers) biogeochemical processes by simulating the cycling of phytoplankton growth
174 (two different groups) using light, temperature, and nutrient availability. Simulations were run
175 using previously-used temperature optima for the growth of both phytoplankton groups (Testa et
176 al., 2014), and we tested these formulations against simulations where elevated temperature
177 would not limit phytoplankton growth (see Supplemental Material). RCA simulates oxygen,
178 carbon, nitrogen, phosphorus, silica, and sulfur dynamics, and we used initial sediment
179 porewater and solid concentrations that were generated from a 5-year "warm-up" (see Testa et
180 al., 2014). Detailed descriptions of ROMS-RCA and the sediment biogeochemical model (SFM)
181 and their parameters can be found in recent publications (Brady, Testa, Di Toro, Boynton, &
182 Kemp, 2013; Li et al., 2016; Ni et al., 2019; Shen et al., 2019; Testa et al., 2014) and we report
183 mean concentrations of relevant model state variables in the Supplemental Material from our
184 baseline model runs.
185
186 *Sensitivity simulations*: Sensitivity simulations were performed using three years with different
187 hydrologic regimes to allow for the quantification of the impacts of different physical regimes on
188 the estuary's sensitivity to altered temperature and nutrient load timing. The years include an
189 above-average river flow year (2004), a below-average river flow year (2002), and a moderate,
190 or average flow year (2000; Fig. 2). For warming simulations, we only elevated temperature in
191 the biogeochemical model to isolate the biogeochemical effects of the warming on hypoxia.

192 *Nutrient Timing Scenarios:* For each of the three hydrologic conditions (2000, 2002, and 2004), the
193 average of all major tributary NO_{23} concentrations (i.e., concentrations in the river load) was
194 used to generate an idealized annual cycle. We focused on NO_{23} because it is typically >70% of
195 the TN load (Zhang, Brady, Boynton, & Ball, 2015) and is the dominant source of nitrogen that
196 reaches downstream areas to support algal growth Chesapeake Bay (Palinkas, Testa, Cornwell,
197 Li, & Sanford, 2019). This annual cycle was then scaled to match the nutrient concentration and
198 load magnitude in each individual tributary by multiplying the cross-tributary average annual
199 loading cycle by a tributary-specific factor (i.e., the ratio of the tributary concentration to the
200 watershed-mean concentration). This approach maintained the relative load magnitude from each
201 tributary, but removed tributary-specific seasonal variability in concentrations to establish an
202 identical seasonal variation in concentration for each tributary to allow for the isolation and
203 simplification of the timing effect. This approach comprised the 'idealized Base' (no change)
204 scenario for comparison to suite of altered nutrient concentration timing simulations. For each
205 hydrologic year, two additional model scenarios were performed that consisted of shifting the
206 idealized tributary (riverine) nitrate + nitrite concentration earlier in the year (1 and 2 months
207 earlier), for each of the major tributaries modeled. Thus, the NO_{23} timing scenarios consisted of
208 three different model simulations: (1) an idealized 'Base' scenario where no changes in NO_{23}
209 were applied, and two 'shift' scenarios where the peak NO_{23} concentration is shifted (2) one and
210 (3) two months early (Fig. 3). Although the potential for this particular type of shift in nitrogen
211 concentration to be realized in Chesapeake Bay watershed is unclear, numerous studies in other
212 regions have projected that future climates will alter the seasonality of nutrient loads (Bouraoui,
213 Grizzetti, Granlund, Rekolainen, & Bidoglio, 2004), including shifts to larger winter loading
214 proportions (Marshall & Randhir, 2008; Verma et al., 2015).

Summer Water Temperature Increase Scenario: We performed sensitivity simulations to understand the seasonally-specific response of Bay biogeochemistry to elevated temperatures. While climate projections typically predict that water temperature increases will occur across all months of the year (Ni et al., 2019), recent analyses have suggested that late spring and summer temperatures have warmed faster than fall or winter (Hinson, Friedrichs, St-Laurent, Da, & Najjar, 2021; Testa et al., 2018). Therefore, warming was applied by increasing the water temperature by 1.5 °C during the period spanning May 1 to July 31 for each hydrologic year (2000, 2002, and 2004). The temperature increase scenarios were compared to a Base (no change) scenario that included observed nutrient concentrations in riverine inflows.

Nutrient Shift and Summer Water Temperature Increase Combination Scenarios: The effects of earlier nutrient load timing and elevated summer water temperatures are likely to occur simultaneously. Therefore, we conducted simulations of summer water temperature increases of 1.5 °C Bay-wide from May 1 to July 31 combined with shifting the NO_{23} timing 1 and 2 months early respectively for each hydrologic year. These simulations allow for an analysis of interactions between the two climate change-induced alterations of external forcing with reference to the impacts in isolation.

Year-round Water Temperature Increase Scenario: In contrast to the observation of the largest deviations in long-term averages of water temperature occurring in the summer (Testa et al., 2018), other studies have projected year-round water temperature increases in the Chesapeake Bay region (Ding & Elmore, 2015; Ni et al., 2019). To evaluate estuarine sensitivity to potential year-round water temperature increases, we performed a simulation by increasing the water temperature by 1.5 °C, Bay-wide, for the entire year, under the Base loading scenario. This

239 simulation was repeated for each hydrologic year (i.e., 2000, 2002, and 2004). These year-round
240 temperature increases were directly compared to the early summer increases.
241
242 **Results**
243 *Nutrient Timing Scenarios:* At the Bay-wide scale, idealized simulations of earlier nutrient loads
244 resulted in lower annual hypoxic volumes for all hydrologic regimes (Fig. 4). This occurred even
245 as the cumulative NO_{23} load was higher in the nutrient shift scenarios for the wet year, resulting
246 from an alignment of the shift with high January flow in 2004 (Figs 2&3). The simulated
247 reductions in hypoxic volume were comparable across years, with a maximal reduction between
248 1.2 and 1.6 km^3, equating to a 5-10% reduction relative to base conditions (Fig. 4). For all years,
249 the scenario that shifted NO_{23} two months earlier saw a larger reduction in annual hypoxic
250 volume than the one month early shift. We also computed hypoxic volume days (HVD) as an
251 integrated measure of annual hypoxic volume, where $\text{HVD} = \sum_{d=0}^{365} \text{HV}_d$ and d = day of the year
252 and HV = the daily hypoxic volume in the mainstem Bay and its tributaries (km^3). At the
253 hypoxia threshold of 2 mg O_2/L, the two month earlier shift during the moderately wet year
254 (2000) had the largest decrease in HVD with a change of 117.4 km^3-day, followed by 106.4 km^3-
255 day in 2004 (wet), and 75.4 km^3-day in the 2002 (dry) scenario. Although there was no change in
256 the timing of the peak hypoxic volume for any of the scenarios, the reductions were consistent
257 from June to October in the moderate (2000) flow year, between June and September in the dry
258 year, and larger in May to July in the wet (2004) year (Fig. 4). The timing of hypoxia initiation
259 wasn't heavily influenced by the shift in nitrate load timing, and only changed by 1 or 2 days for
260 a region or two in each of the hydrologic years.

The fact that earlier nitrate load timing initiated a decrease in Bay-wide hypoxic volume indicates that these scenarios included an increase in bottom-water dissolved oxygen. We computed the difference in modeled dissolved oxygen, chlorophyll-*a*, and respiration during the spring (January-May) and summer (June-August) in model cells corresponding to three Chesapeake Bay Program monitoring stations along the Bay mainstem including: CB3.3C (Bay Bridge) in the upper Bay, CB5.3 (Smith Point) mid-Bay, and CB6.4 in the lower Bay (Fig. 1). Both the 1- and 2-month shifts in nitrate concentration caused an increase in water column dissolved oxygen that correlated to a decrease in chlorophyll-*a* (see Supplemental Material) and total respiration (DOC oxidation + sulfide oxidation + phytoplankton respiration) during both the spring and summer seasons (Fig. 5). For the moderately wet (2000) and wet (2004) years, the middle and lower-Bay stations saw a larger increase in dissolved oxygen in both seasons compared to the upper-Bay station (Fig. 5). During the driest year (2002), the upper-Bay station showed the largest change in dissolved oxygen during the spring season. In general, the two month earlier nutrient shift had a larger effect on the dissolved oxygen linkage with chlorophyll-*a* and respiration during both seasons than the one month early scenario, by increasing the dissolved oxygen as much as 3 mg O_2/L at the mid-Bay station in the summer. Whereas the one month early nutrient shift scenario generated about a 0.5-1 mg O_2/L at the same station and season.

Remineralization processes in sediments and associated sediment-water fluxes also varied seasonally in response the simulated shift in NO_{23} concentration and load. Comparisons of the NO_{23} shift one month early scenario in all regions showed that modeled sediment oxygen demand (SOD), sediment-water NH_4 flux, and sediment nitrogen all deviated from the 'Base' case beginning in May, continuing through the summer, and then returned to 'Base' case values

between October and November (Figs. 6&7). The one month early nutrient shift scenario actually resulted in enhanced sediment oxygen demand (SOD) in the two upper CBP stations (CB3.3C and CB5.3), and slightly reduced SOD at the lower Bay station (CB6.4) (Fig. 6). Sediment-water NH_4 fluxes peaked during late summer through early fall (July to October), and during this period, the shift NO_{23} one month early scenario shows a reduction in NH_4 release from the sediments of 1-5% except for the wet year (2004) in the upper bay (Fig. 7). Particulate organic nitrogen (PON) in the sediment was also reduced in the nutrient shift scenarios (Fig. 7). For the upper-Bay stations (CB3.3C and CB5.3), this reduction in PON is initiated around March, but was delayed until May in the lower-Bay station (CB6.4; Fig. 7).

Seasonal Water Temperature Increase Scenario: The idealized early summer warming scenarios resulted in an altered annual cycle of dissolved oxygen. Hypoxic volume increased up to 3 km^3 during the period of increased water temperature (May-July), but once warming subsided after July 31, model simulations revealed a slight reduction in hypoxic volume in all hydrologic years (Fig. 8). The associated largest overall (delta) change in HVD occurred during the 2004 scenario with an increase of 108.6 km^3-day, where this year had the largest increase in hypoxia during the temperature increase period and the largest reduction after July 31 time period with a change in HVD of 146.3 km^3-day and -37.6 km^3-day, respectively (Fig. 8). The moderately wet year (2000) had the largest lag after July 31 for hypoxia to decrease below the Base scenario at 10 days, whereas the dry and wet years responded in 7 and 4 days respectively (Fig. 8).

The seasonal response of hypoxia to temperature increases was driven by changes in water-column and sediment respiration. SOD and water-column respiration uniformly increased under warming in the middle and lower Bay, except for the wet year, 2004, when both rates

307 declined with elevated temperature in the middle Bay (Fig. 9). In contrast, SOD and water-
308 column respiration were reduced or changed minimally under warming in the upper Bay (Fig. 9).
309 In the week leading up to the end of the warming on July 31 and in the month after, sediment
310 respiration (SOD) declined in the middle and lower Bay, which corresponded to the reduction in
311 available sediment organic carbon (SOC), which never recovered to levels from the Base case
312 within the remainder of the year (Fig. 10). The upper-Bay station (CB3.3C) saw the largest
313 reduction in SOC (up to ~0.15 mg C m^{-3} in moderate and dry year; Fig 7) relative the middle and
314 lower Bay, but SOD reductions in the mid-late summer were larger in the middle and lower Bay
315 (Fig 9a). We compared the relative contribution of sediment and water column respiration to
316 total respiration in middle and lower Bay regions when both rates were enhanced under warming
317 (May-July in Fig.9), where we assumed a 10 meter sub-pycnocline water-column. If we consider
318 an enhancement of water-column respiration by 0.01 mg O_2/m^3-d, which is at the low end of the
319 May-July increases in the middle and lower Bay (Fig. 9b), sub-pycnocline respiration would
320 equal 0.1 mg O_2/m^2-d, which is comparable to the enhancement in SOD (Fig. 9). Thus, a reduced
321 SOC pool following spring warming was associated with reduced water-column and sediment
322 respiration in the fall, which was consistent with the Bay-wide decrease in fall hypoxic volume
323 in the warming scenario.
324
325 *Nutrient Shift and Water Temperature Increase Combination Scenarios:* The combined scenario
326 of earlier nutrient input timing and summer temperature increases resulted in an increase in
327 hypoxic volume (at threshold of 2 mg O_2/L) during the first half of the year (before July 31) and
328 decrease in hypoxic volume in the second half of the year (after July 31) for both scenarios and
329 for all hydrologic years (Fig. 11). The summer temperature increase only scenario had the largest

hypoxic volume increase (11-25%) in the first half of the year and smallest (reduced volume) change (-1 to -4%) in the second half of the year. The combined nutrient shift + summer temperature increase scenarios had smaller increases (shift 1-month early=8-18%, shift 2-months early=5-13%) than the temperature-only increase, and larger decreases in hypoxic volume in the latter half of the year relative to temperature increases only (shift 1-month early= -3 to -7%, shift 2-months early= -8 to -12%; Fig. 11). Separate computations of HVD indicated that summer temperature increases had a sufficient stimulatory effect on hypoxia to overcome reductions resulting from an earlier NO_{23} load. The shift NO_{23} 1-month early scenario had a reduction of 3-6% across all three hydrologic years, whereas the combined warming and NO_{23} 1-month early shift scenario had a 2-10% increase. The shift NO_{23} 2-months early scenario had larger reductions in volume of 5-12% across all three hydrologic years, while the comparable combined scenario had a 3% reduction in 2000, 3% increase in 2002, and negligible change (0.05%) in 2004.

Year-round Water Temperature Increase Scenario: The year-round temperature increase scenario caused elevated hypoxic volumes (at threshold of 2 mg O_2/L) in comparison to the Base (no change) scenario throughout the year. These increases were comparable in 2000 (by 18%) and 2002 (by 17%) and somewhat smaller for 2004 (by 8%; Fig. 11). This increase in hypoxic volume was larger than the summer temperature increase scenario, which had a 10, 15, and 5% increase for 2000, 2002, and 2004 respectively. In the year-round increase scenarios, both 2002 and 2004 showed a slight decline in hypoxic volume around October, but it was relatively small in comparison to the overall increase. The late fall decrease in the two warming scenarios was of similar magnitude, but is shifted about a month later in the year-round warming scenario. Across

353 all years, the early summer (before July 31) increase in volume was comparable to the summer
354 water temperature increase only scenario. One difference observed was during 2004, when the
355 increase in hypoxic volume occurred much earlier in the year than all other temperature
356 scenarios (Fig. 11).
357
358 **Discussion**
359 The phenological response of estuaries to changes in climate and watershed nutrient
360 loading is complex and can be subtle, but model simulations (e.g. ROMS-RCA) were able to
361 quantify the effects of seasonal changes to external forcing on oxygen depletion. Here, we
362 documented responses of Chesapeake Bay hypoxia to two distinct changes in the seasonal timing
363 of physical forcing. Shifts in nutrient load timing had the effect of reducing the overall annual
364 hypoxic volume in response to declines in phytoplankton biomass and both sediment and water-
365 column respiration in three regions of the Bay. Seasonally-specific and annual-scale water
366 temperature increase scenarios indicated an increase in the spring/early summer hypoxic volume,
367 but a decrease in late summer/fall hypoxic volume. In combined load timing-warming
368 simulations, warming outweighed load timing in its effect of increasing hypoxic volume. Each of
369 these idealized simulations represents a potential future change to Chesapeake Bay associated
370 with either a direct (temperature) or indirect (nutrient load timing) response to future climate
371 warming, and the simulations highlight the complex metabolic response to external forcing that
372 drives responses in hypoxic volume.
373 Previous studies have shown how annual or long-term scale reductions in nutrient load
374 are linked to reductions in stream nutrient concentrations (Ator, Blomquist, Webber, & Chanat,
375 2020; Eshleman, Sabo, & Kline, 2013) and lead to improvements in dissolved oxygen (Fisher et

al., 2021), the recovery of submerged aquatic vegetation (Greening & Janicki, 2006; Lefcheck et al., 2018), the reduction in sediment nutrient cycling (Taylor et al., 2020), and other ecosystem responses (Fulweiler, Nixon, Buckley, & Granger, 2007; Riemann et al., 2015). This study suggests that reductions in hypoxia might also occur as a result of seasonal shifts in nutrient load timing (Fig. 4). Although the idealized shifts in nutrient timing we simulated may be more extreme (e.g., 2-month shift) than changes resulting from fertilizer application or forest phenology (Elmore et al., 2016), the oxygen response we found may be an overlooked potential effect of changes in watershed nitrogen export on estuarine biogeochemistry. A large portion of the Chesapeake Bay watershed is occupied by agricultural landscapes, contributing a large source of estimated nutrient load (42% nitrogen, 55% phosphorus; Chesapeake Bay Program, 2015). Thus, farmer adaptations to changing climate conditions by adjusting agricultural practices to maintain crop yield (Ortiz-Bobea, Wang, Carrillo, & Ault, 2019) is worth considering in future climate scenarios, because it's estimated to lead to earlier nitrate (NO_3) loading (kg/ha) to waterbodies (Chang, Wilusz, & Harman, 2018). By shifting nutrient load timing earlier, NO_{23} availability is reduced during a key period of phytoplankton production (e.g., winter-spring), which means that there would be less organic material available for hypoxia generation later in the year (Boynton & Kemp, 2008; Testa & Kemp, 2014).

Freshwater flow is a strong driver of nutrient loading to estuaries and river flow moderated the spatial response of hypoxia and metabolism to idealized changes in load timing. The Susquehanna River is the dominant source of freshwater and nutrients to the mainstem Chesapeake Bay, correlating strongly with the magnitude of annual hypoxia in estuaries (Li et al., 2016; Scavia, Kelly, & Hagy, 2006) and water-column chlorophyll-*a* accumulation (Miller & Harding, 2007). Model scenario results highlight this flow effect regardless of the nutrient timing

399 or temperature scenario, where the relative change in Bay-wide hypoxic volume was largest in
400 the highest flow (and hypoxic volume) year for the one-month shift (2004) and highest in the
401 moderate flow year (2000) for the two-month shift (Fig. 4). The spatially-specific responses of
402 other variables was distinct, including a larger reduction in NH_4 fluxes and sediment PN and PC
403 during the moderate and low flow years in the upper Bay. This high sensitivity of the upper Bay
404 is consistent with high flow conditions that push the spring bloom and associated organic matter
405 deposition seaward (Testa et al., 2014) and thus the upper-Bay had little biogeochemical
406 production and sensitivity to load changes in the wet year of 2004. The lower Bay, in contrast,
407 had the strongest metabolic response to nutrient load timing changes, revealing the dependence
408 of primary production and associated metabolism to Susquehanna River nutrient inputs in this
409 region (Miller & Harding, 2007; Testa et al., 2018).
410 An unexpected result of the simulations was the apparent stimulation of SOD and water-
411 column respiration with altered nutrient input timing and reduced hypoxia. This feature was
412 especially evident in the upper Bay in the moderate and dry year, the middle Bay in the moderate
413 and high flow year, and the lower Bay during the wet year (Fig. 6). This result reflects the fact
414 that respiration (and associated oxygen uptake) can be limited by oxygen availability (Cowan &
415 Boynton, 1996; Sampou & Kemp, 1994). Thus in the upper and middle-Bay, where oxygen
416 concentrations in bottom waters under the base scenario are anoxic or severely hypoxic, SOD
417 and water-column respiration are oxygen limited. Therefore, when the nutrient shifts reduced
418 oxygen consumption and increased oxygen concentration due to reduction of chlorophyll-*a* and
419 total respiration (Figs. 5, 6, S1), oxygen limitation was relieved and SOD increased. The fact that
420 respiration increased when oxygen was made available, but not to an extent to elicit a feedback

421 that would generate the same volume hypoxia for a lower nutrient load, underscores the fact that
422 nutrient reductions, independent of their timing, serve to limit consumption of oxygen.
423 Many previous studies have examined long-term changes in hypoxic volume in estuaries
424 (Carstensen, Andersen, Gustafsson, & Conley, 2014; Hagy et al., 2004; Murphy et al., 2011;
425 Scavia et al., 2006), including simulated responses to future climate change (Cai et al., 2021;
426 Irby et al., 2018; Laurent et al., 2018; Meier et al., 2011; Ni et al., 2020). Fewer studies,
427 however, have examined detailed metabolic responses that exert influences on changes in
428 hypoxic volume (Li et al., 2016; Testa et al., 2021). Murphy et al. (2011) reported significant
429 increases in early summer hypoxia and a slight decrease in late summer hypoxia in Chesapeake
430 Bay over a 60-year period, where climate-related variables (e.g., elevated stratification) were one
431 explanation for the early-summer increase. Other studies have shown how increases in water
432 temperature are likely to increase the annual hypoxic volume in the Bay (Irby et al., 2018; Ni et
433 al., 2019), or have already mitigated nutrient reduction (Frankel et al., 2022; Ni et al., 2020),
434 through warming-enhancements of respiration and/or reductions in oxygen solubility. In contrast,
435 this study suggests that increases in hypoxic volume in the early part of the year can result from
436 an increase in the early summer temperature, which can be followed by a subsequent decrease in
437 later summer/early fall hypoxic volume (Fig. 11). Testa et al. (2018) hypothesized that warmer
438 early summer temperatures would stimulate the respiration of the spring bloom to generate early
439 summer hypoxia increases, but also exhaust organic matter earlier in the year and allow for late-
440 season relief from hypoxia due to lower late summer respiration rates. The model simulations we
441 performed are consistent with that hypothesis, where the seasonal temperature change lead to a
442 faster rate of sediment and water-column respiration in the early summer, and when temperature
443 returned to observed levels, there was less sediment organic matter to support respiration and

444 nutrient fluxes (Fig. 11). Thus, the impacts of future climate changes may not simply lead to
445 higher hypoxia, but rather increase hypoxia in early summer and decrease it in later summer, as
446 has been previously documented (Murphy et al., 2011; Testa et al., 2018; Zhou, Scavia, &
447 Michalak, 2014). The fact that the year-round warming scenario generated a smaller late summer
448 hypoxia decline than the summer-only temperature increase scenario (except 2002 with a 15-
449 17% increase; Fig. 11) reinforces that the extent and seasonality of warming will modulate the
450 realization of any proposed alteration of seasonal hypoxia cycles. Thus, although temperature
451 increases may indeed lead to a more rapid respiration of labile organic material in the early part
452 of the annual cycle, temperature increases across all times of year will extend a larger hypoxic
453 volume into the mid to late fall in Chesapeake Bay.

454 These idealized simulations appear to support the hypothesis that temperature increases
455 can have complex, spatially and seasonally-dependent effects on hypoxia. Some of these effects
456 may be realized through recycling-associated feedbacks (Savchuk, 2018; Testa & Kemp, 2012),
457 which we did not fully explore here. For example, warming-induced increases in respiration
458 (Yvon-Durocher, Jones, Trimmer, Woodward, & Montoya, 2010) would allow for elevated
459 regeneration of nutrients in the water-column and sediments (Lake & Brush, 2015), which could
460 stimulate additional phytoplankton production during summer and add additional organic
461 material later in summer to compensate for the material exhausted by warming. Indeed, a 10-
462 20% increase in water column NH_4 in both the surface and bottom waters occurred under
463 warming in our simulations, which could support additional phytoplankton growth. Although
464 this regeneration of nitrogen is relatively strong during the summer temperature increase, the
465 effect did not persist long into the fall, and therefore was unable to sustain further phytoplankton
466 production in the model simulations.

The combined scenarios of earlier nutrient load timing and warmer water temperature showed that the reduction in hypoxic volume generated by the shift in nutrient load timing is overcome by the increase in summer water temperature. This result indicates that although organic matter reductions through lowered primary production under earlier nutrient inputs will reduce the respiration that generates hypoxia, elevated respiration rates of the existing organic material and reduced oxygen solubility will increase hypoxia. This is consistent with simulations that have shown that temperature effects will limit the oxygen improvements expected from nutrient load reductions in Chesapeake Bay (Du, Shen, Park, Wang, & Yu, 2018; Irby et al., 2018; Ni et al., 2020) and other estuaries (Meier et al., 2011; Whitney & Vlahos, 2021). However, the reduction in later summer hypoxia associated with warmer summer temperatures persists with the addition of earlier nutrient inputs, and the reduction in hypoxic volume was larger in the combined nutrient shift + warming scenarios for 2000 and 2002 than the summer temperature increase scenario alone (and was comparable across years; 4-8%). Thus, the combination of these two likely climate change effects on external forcing could lead to an altered seasonality of hypoxic volume. These seasonal alterations are potentially relevant for mobile and sessile organisms that have seasonally-specific recruitment and migration patterns, and whose habitat may be limited by reduced dissolved oxygen (O_2) levels more than high temperature during summer months (Kraus, Secor, & Wingate, 2015).

The model simulations presented here provide new insights into the potential alteration of biogeochemical phenology in Chesapeake Bay and other estuaries, but the idealized simulations do have limitations. First, future simulations could include more realistic temperature changes from downscaled model simulations and account for other effects of climate change, including changes in the timing and variability of freshwater discharge. Our application of three different

hydrologic years in our simulations was advantageous because it allowed for the simulation of changes only in nutrient concentration under natural hydrological conditions. The disadvantage of this approach is that future climate in this region is expected to include both warming and elevated flow, and also that differences in flow seasonality within the years we simulated caused an increase in nitrogen load in some scenarios (Fig. 3), but even in this case the phenology shift appeared to persist (e.g., Fig. 5). Furthermore, the 2-month shift in nutrient concentration scenario is likely an extreme case, but we included this run to provide an upper bound to the potential effect of altered load timing. We also did not explore potentially co-occurring impacts on phosphorus, which is a key limiting nutrient in spring (Zhang et al., 2021), and future efforts could consider changes in the N:P ratio. Finally, the scenarios including warming combined with nutrient load timing changes represent perhaps the most realistic case of future conditions, as future warming is the presumed cause of any shifts in nutrient load timing.

Conclusion and Future Recommendations

Targets for watershed nutrient load reductions are typically evaluated on an annual basis, but the results of idealized model simulations presented here indicate that even when the annual load remains stable, intra-seasonal dynamics in loading may also impact hypoxic volumes. Future changes in the timing of agricultural activity and associated stream nutrient concentrations – including changes in practices that occur in response to climate changes – will have cascading effects on the estuary. These idealized seasonal simulations and the hypoxia responses displayed that earlier nutrient timing can limit the extent of hypoxic volume, but that warming can overwhelm these effects. The reduction in hypoxic volume due to the decoupling of nutrient load and seasonal water temperature would not be as strong if water temperatures

continue to warm earlier in the spring, expanding the seasonal overlap of high nutrient loading and high metabolic rates. These outcomes would be further modulated by other future climatic changes, including altered wind patterns, sea level rise, and changes in the biological communities within the plankton.

Making future projections with a biogeochemical model can be challenging, because the model kinetic formations are inflexible and are limited by the science available to inform model formulation, parameterization, and the inclusion of all relevant biological and biogeochemical interactions. For example, future climate changes will likely alter phytoplankton species abundance and distribution, but the current biogeochemical model only represents two idealized functional types (a summer group and a winter diatom group). Given that these models do not represent a dynamic and flexible community of different phytoplankton types and metabolic modes, the model will have a limited capability to accurately predict the varied potential outcomes for phytoplankton metabolism. Phytoplankton kinetics, including nutrient uptake and respiration could play a large role in ecosystem nutrient cycling under climate change. Overall, this study illustrates how alterations in the phenology of human behavior, physical forcing, and biogeochemistry can potentially be important when studying climate change effects on Chesapeake Bay and other estuaries. Future simulations with more comprehensive watershed-estuarine model coupling are necessary to more confidently evaluate the potential for these altered realizations of hypoxia to occur. For examples, the effects of warming and altered precipitation patters on watershed nitrogen cycling (Wagena et al., 2018), nitrogen speciation (Bertani, Bhatt, Shenk, & Linker, 2021), and estuarine nutrient cycling will impact any future estuarine responses in terms of nutrient loading and its impacts on oxygen depletion, phytoplankton growth, and nutrient cycling. While the scenarios presented here are simplistic

and somewhat hypothetical, they lend insights into the potential cascading effects of phenological changes within the watershed and estuary and warrant further study.

Additional supporting information may be found online under the Supporting Information tab for this article. This document includes figures, tables, and text to describe (a) model sensitivity tests regarding algal growth formulations, (b) additional analysis of chlorophyll-a and dissolved oxygen concentrations, and a summary of baseline model concentrations and process rates.

Acknowledgements

We would like the thank the many state and federal agencies who collected and processed the datasets used in this analysis, including the Maryland Department of Natural Resources, the Virginia Department of Environmental Quality, the US EPA Chesapeake Bay Program, and the United States Geological Survey. This work was supported by grants from the National Science Foundation (CBET-13606395) and National Oceanic and Atmospheric Administration (NA18NOS4780179). This is the University of Maryland Center for Environmental Science Publication #6231and Ref. No. [UMCES] CBL2023-027.

Data Availability Statement

The data that support the findings of this study are available from the corresponding author upon reasonable request.

le request.

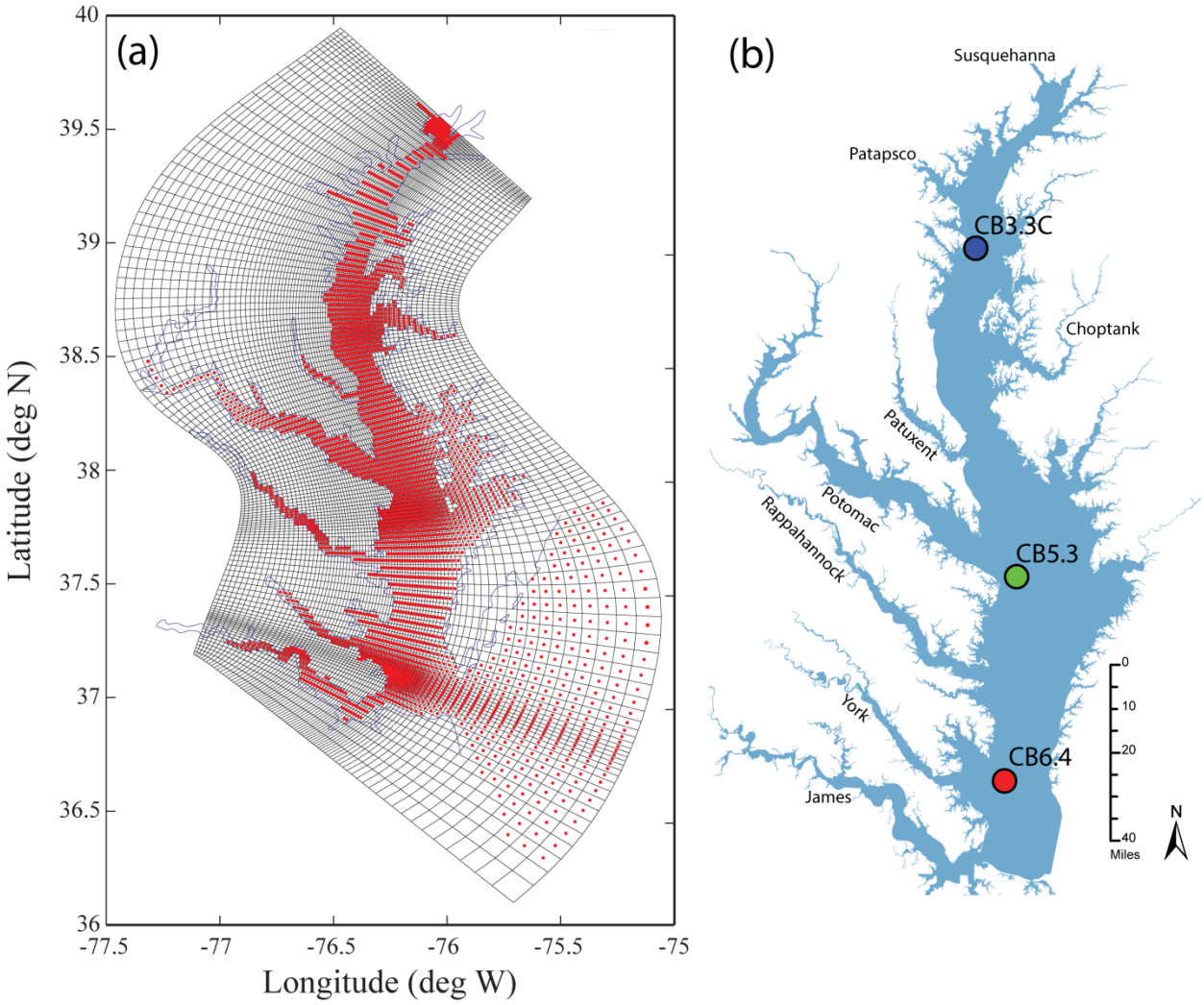

Figure 1: (a) Chesapeake Bay ROMS-RCA model grid (water cells = red) and (b) Map of Chesapeake Bay's major tributaries and the Chesapeake Bay Program long-term water quality monitoring stations (CB3.3C, CB5.3, and CB6.4) that correspond to example locations for analysis in the upper, middle, and lower Bay, respectively.

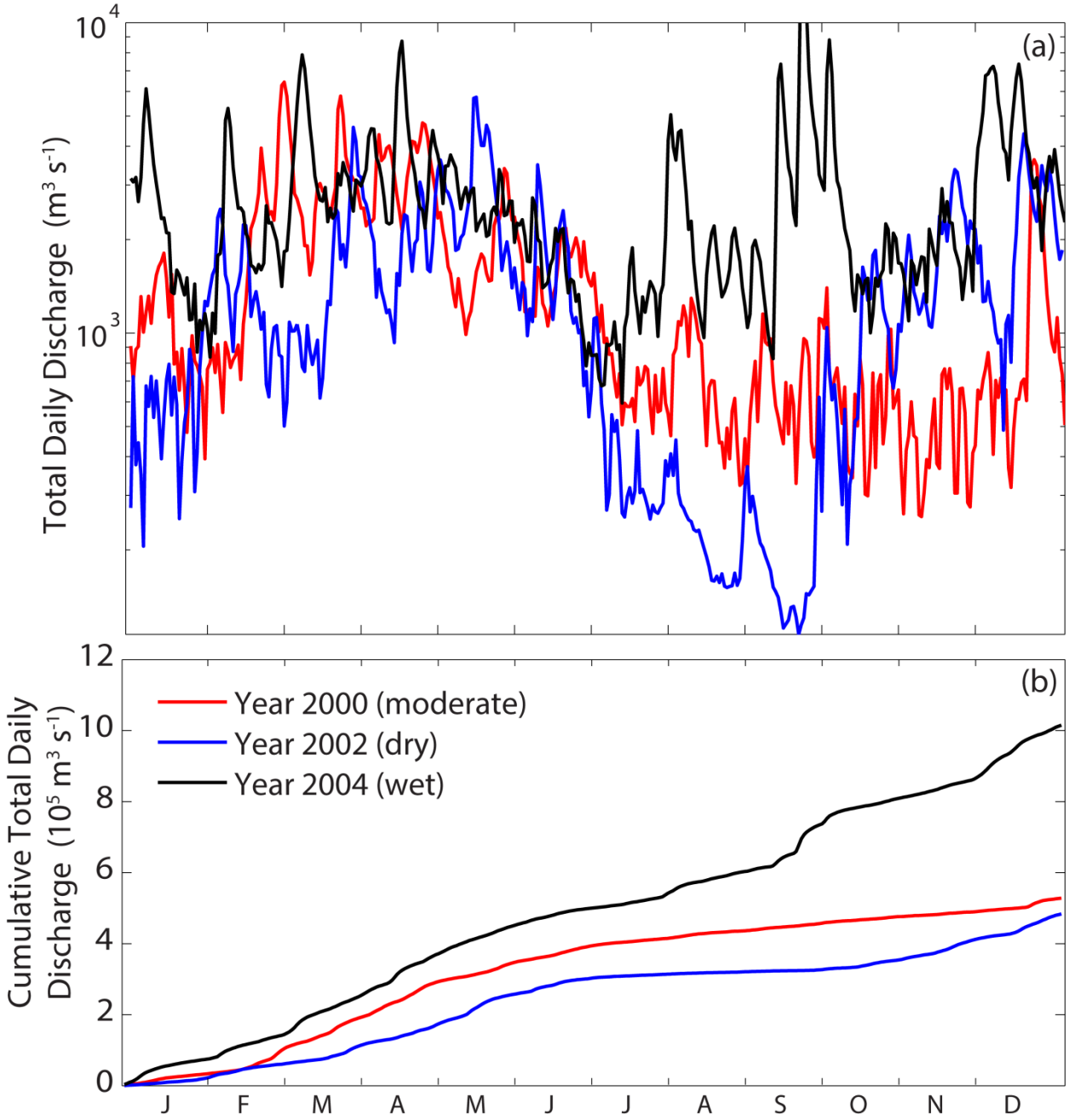

Figure 2: Comparison of the daily total riverine flow (a) and cumulative daily riverine flow (b) of all major Chesapeake Bay tributaries (Susquehanna, Patuxent, Patapsco, Potomac, Choptank, Rappahannock, York, and James Rivers) to highlight that the years 2000 (moderate flow), 2002 (dry), and 2004 (wet) are hydrologically different.

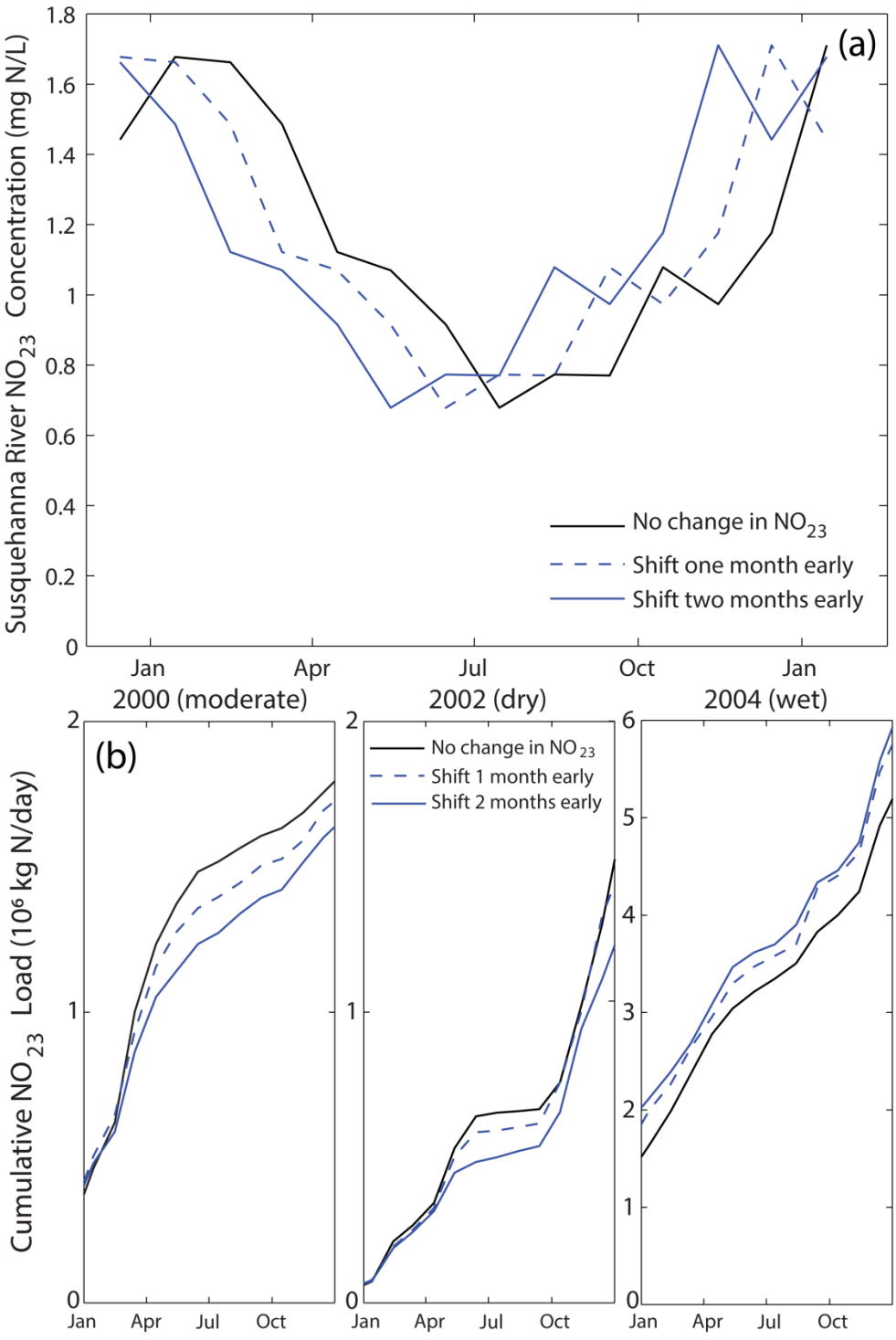

Figure 3: (a) An example of the nutrient load timing shift scenarios for the seasonal concentration of nitrate and nitrite (NO_{23}) shifted to a peak one month early (dashed) and two months early (blue) for the Susquehanna River in 2000. This process was repeated for each hydrological year (2000, 2002, 2004) and tributary. (b) The resulting cumulative NO_{23} load of all tributaries combined, for each year and scenario.

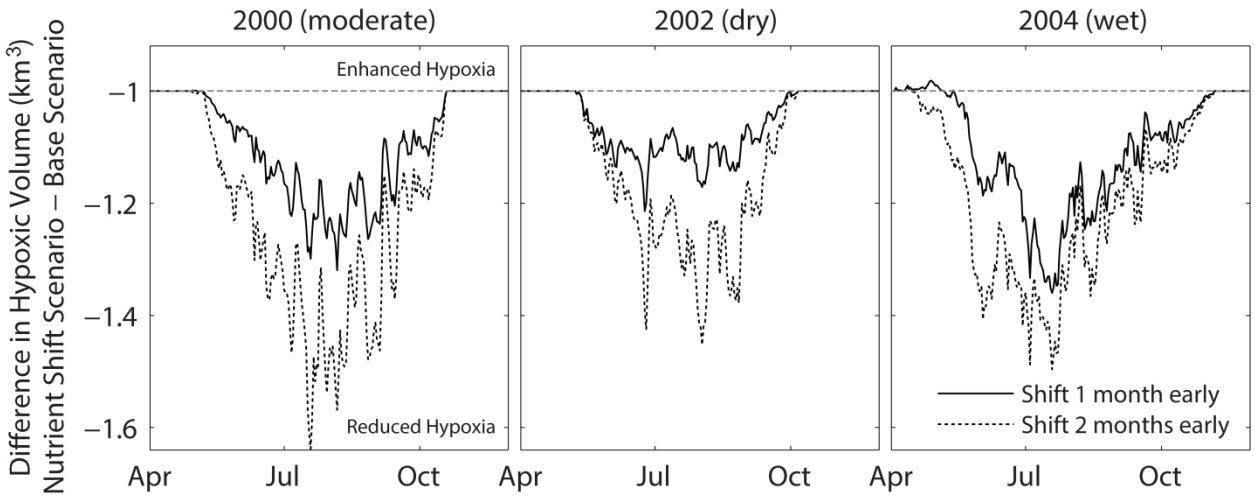

Figure 4: Comparison of the difference between modeled mainstem Chesapeake Bay hypoxic volumes (<2 mg O_2/L) in the nutrient load (NO_{23}) shift scenarios and the baseline simulation (Nutrient Shift-Base) in each year 2000, 2002, and 2004.

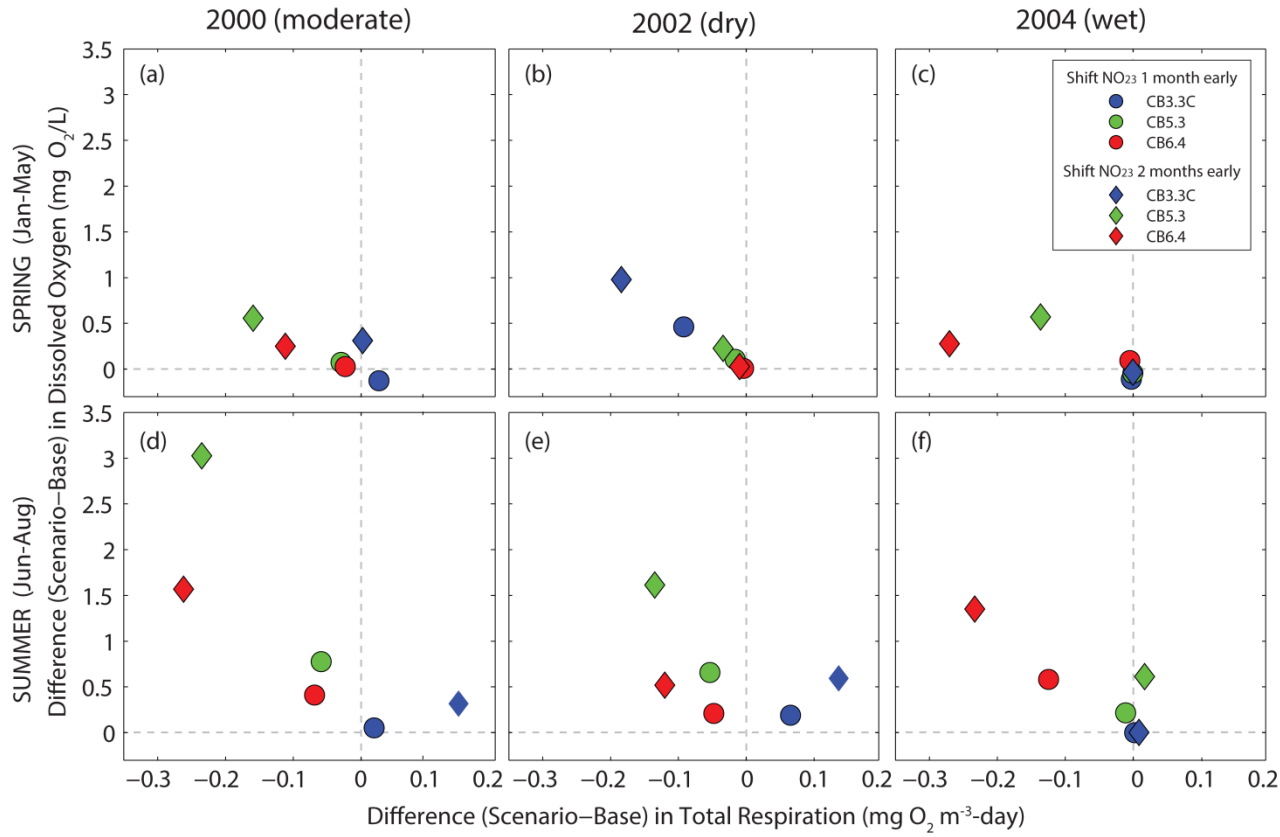

Figure 5: Comparison of the difference in bottom layer dissolved oxygen (O_2) and total respiration respectively, between nutrient timing shift scenarios during the spring (January-May; a-c) and summer (June-August; d-f) seasons at three locations that represent the upper Bay (CB3.3C), the middle bay (CB5.3), and the lower Bay (CB6.4).

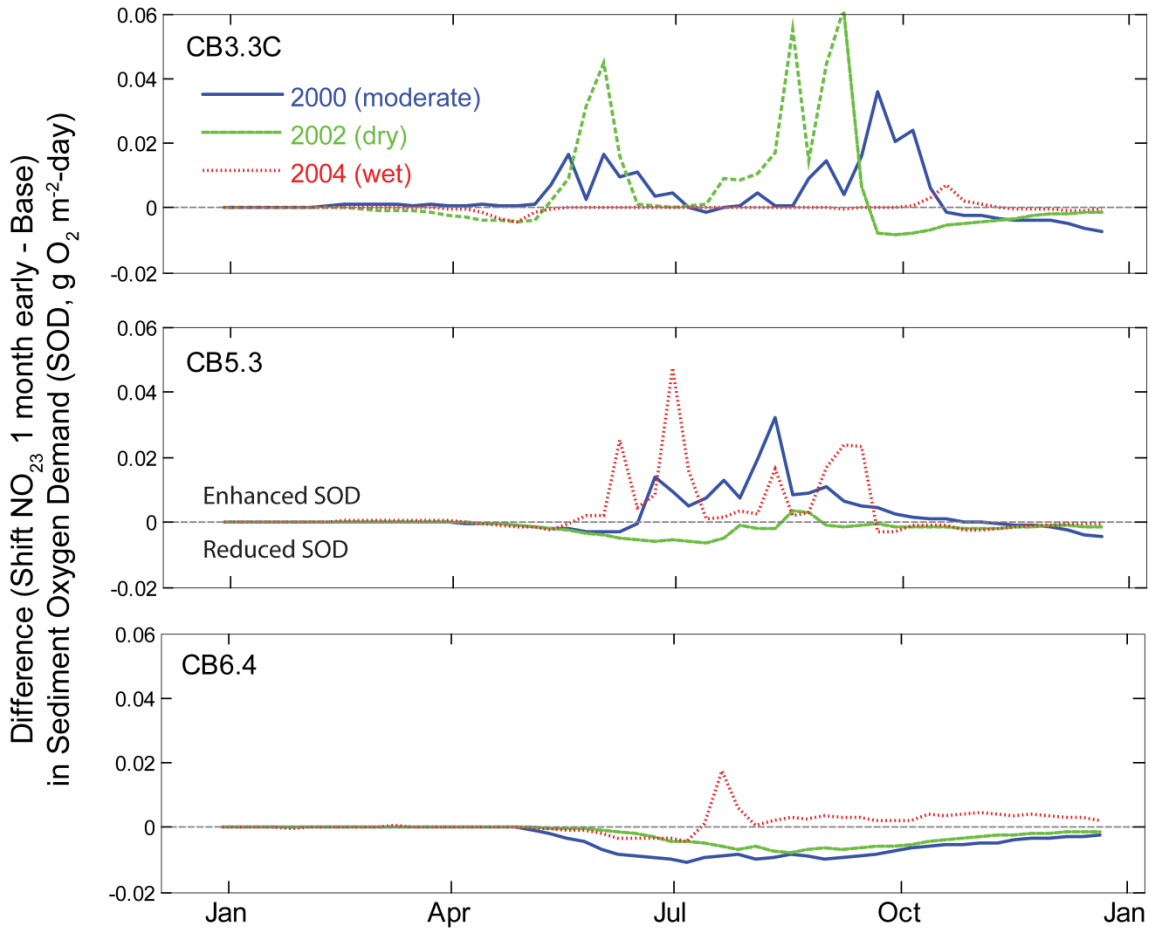

Figure 6: Model-simulated differences (Nutrient shift scenario-Base scenario) in sediment oxygen demand (SOD) for the one-month shift in NO_{23} concentration at three locations that represent the upper Bay (CB3.3C), the middle bay (CB5.3), and the lower Bay (CB6.4). Each of the three hydrologically unique years are included (2000, 2002, 2004).

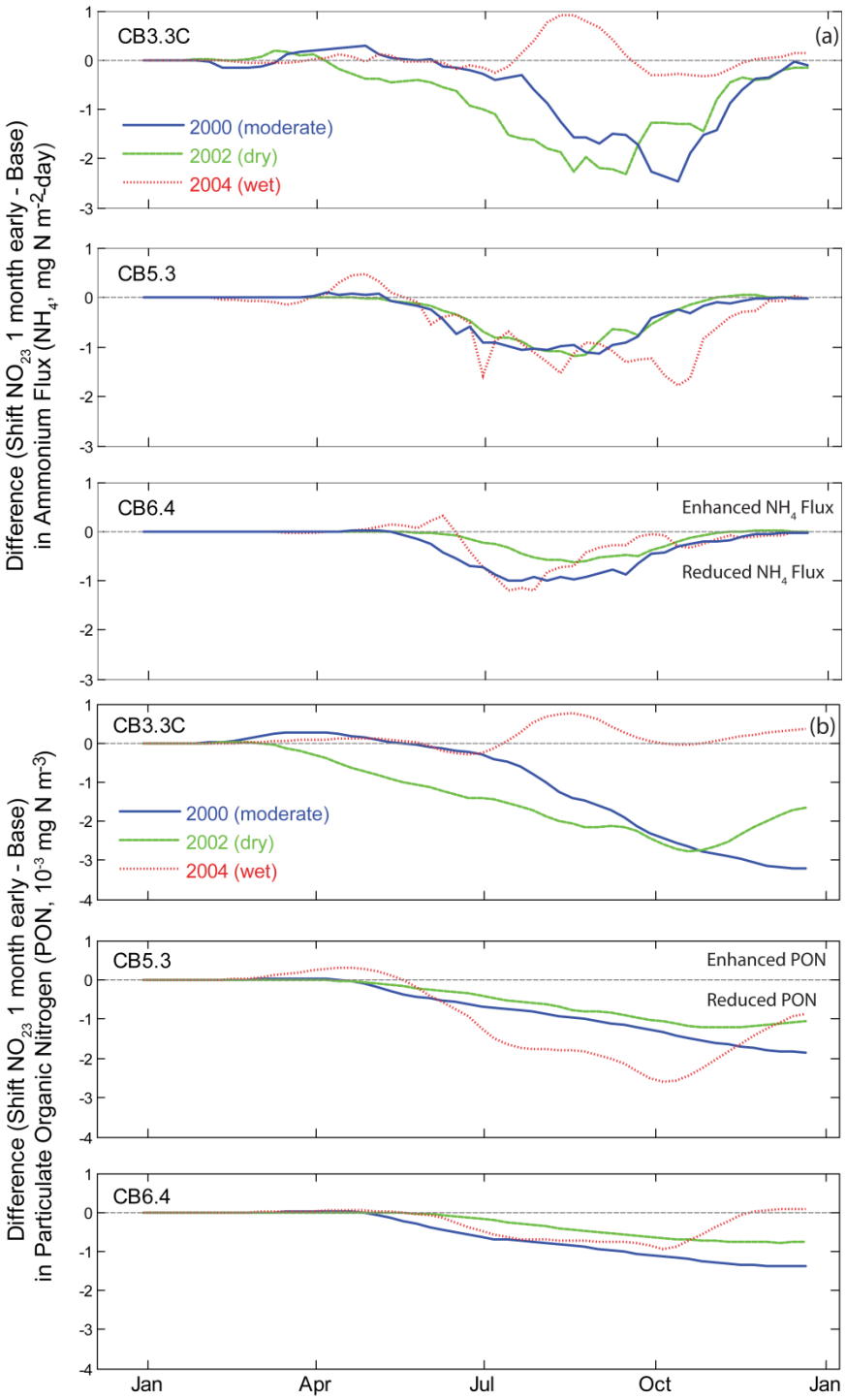

644
645
646 Figure 7: Model-simulated differences (Nutrient shift scenario-Base scenario) in sediment water
647 NH_4 flux (a) and sediment Particulate Organic Nitrogen concentration (PON, b) for the one-
648 month shift in NO_{23} concentration at three locations that represent the upper Bay (CB3.3C), the
649 middle bay (CB5.3), and the lower Bay (CB6.4). Each of the three hydrologically unique years
650 are included (200, 2002, 2004).

651

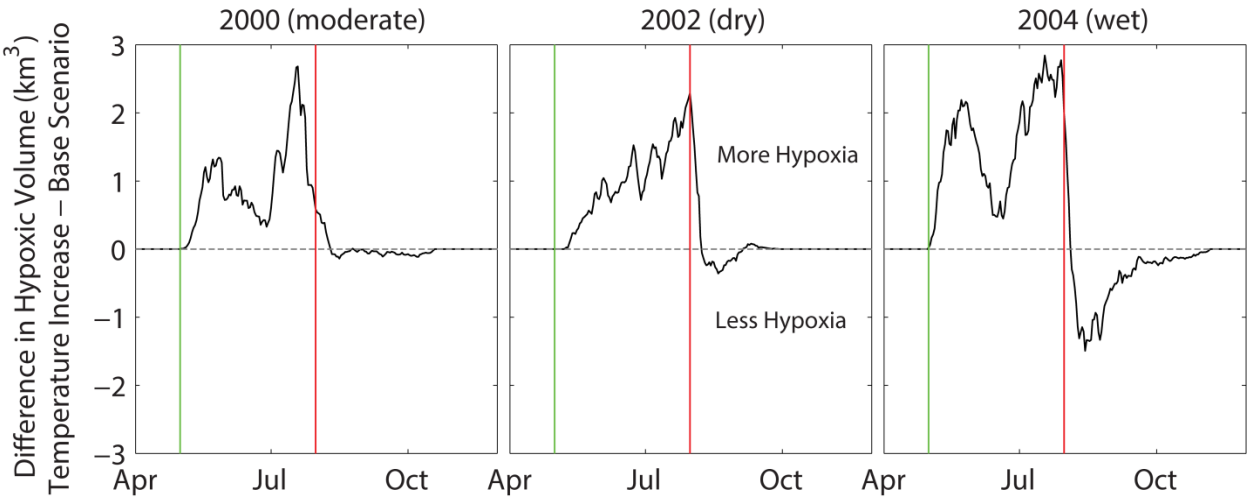

Figure 8: Seasonal difference (warming-Base) in modeled mainstem hypoxia (<2.0 mg O_2/L) in each of three hydrologic years in response to idealized, seasonally-distinct water temperature increase (warming) scenario, where water temperature was increased Bay-wide by 1.5 °C from May 1 (start, green line) to July 31 (stop, red line).

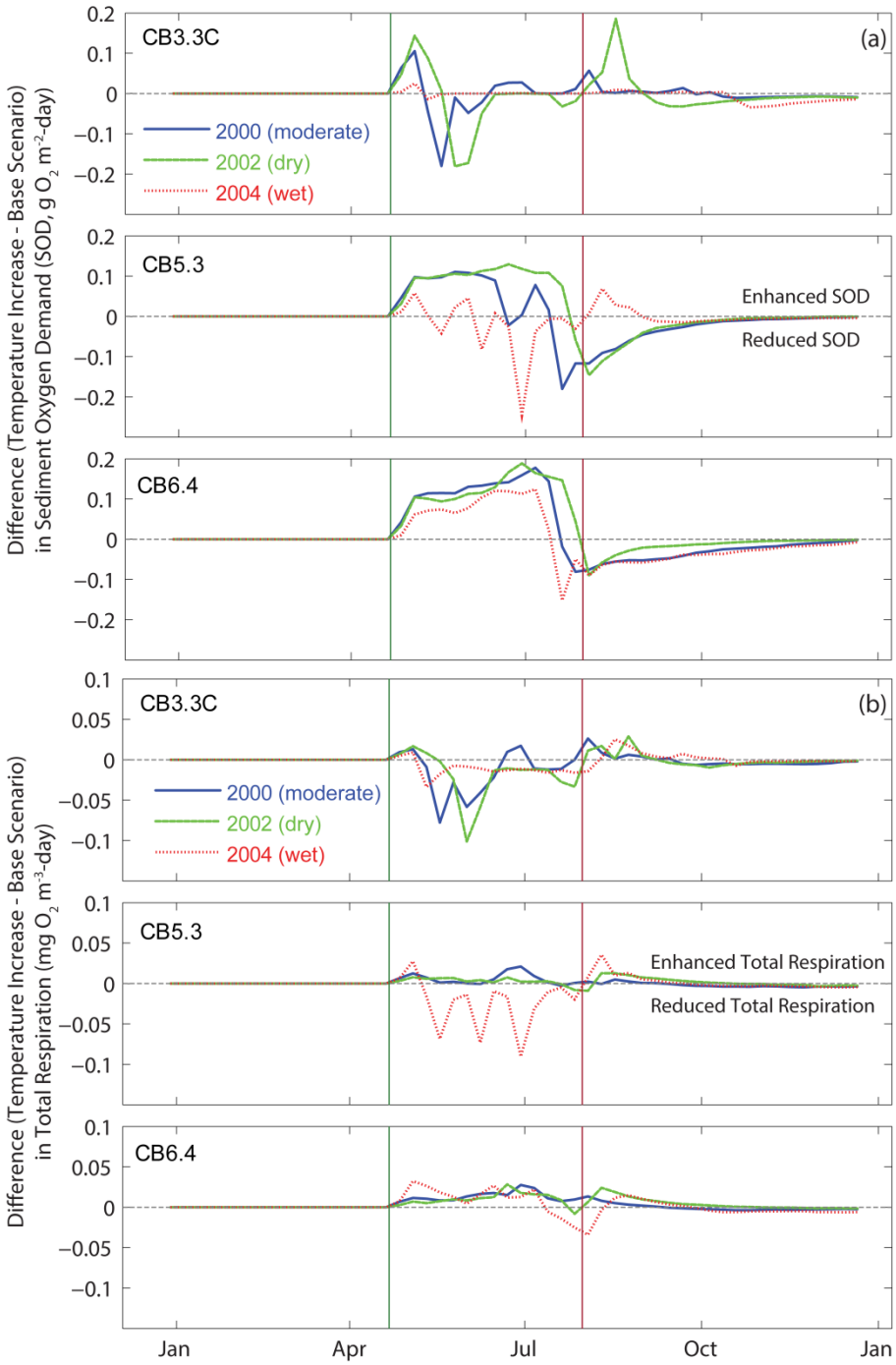

Figure 9: The difference in (a) sediment oxygen demand (SOD) and (b) total respiration between the seasonally-distinct temperature increase scenario and the Base scenario in the upper Bay (CB3.3C), the middle bay (CB5.3), and the lower Bay (CB6.4). The water temperature was increased Bay-wide by 1.5°C from May 1 (start, green line) to July 31 (stop, red line).

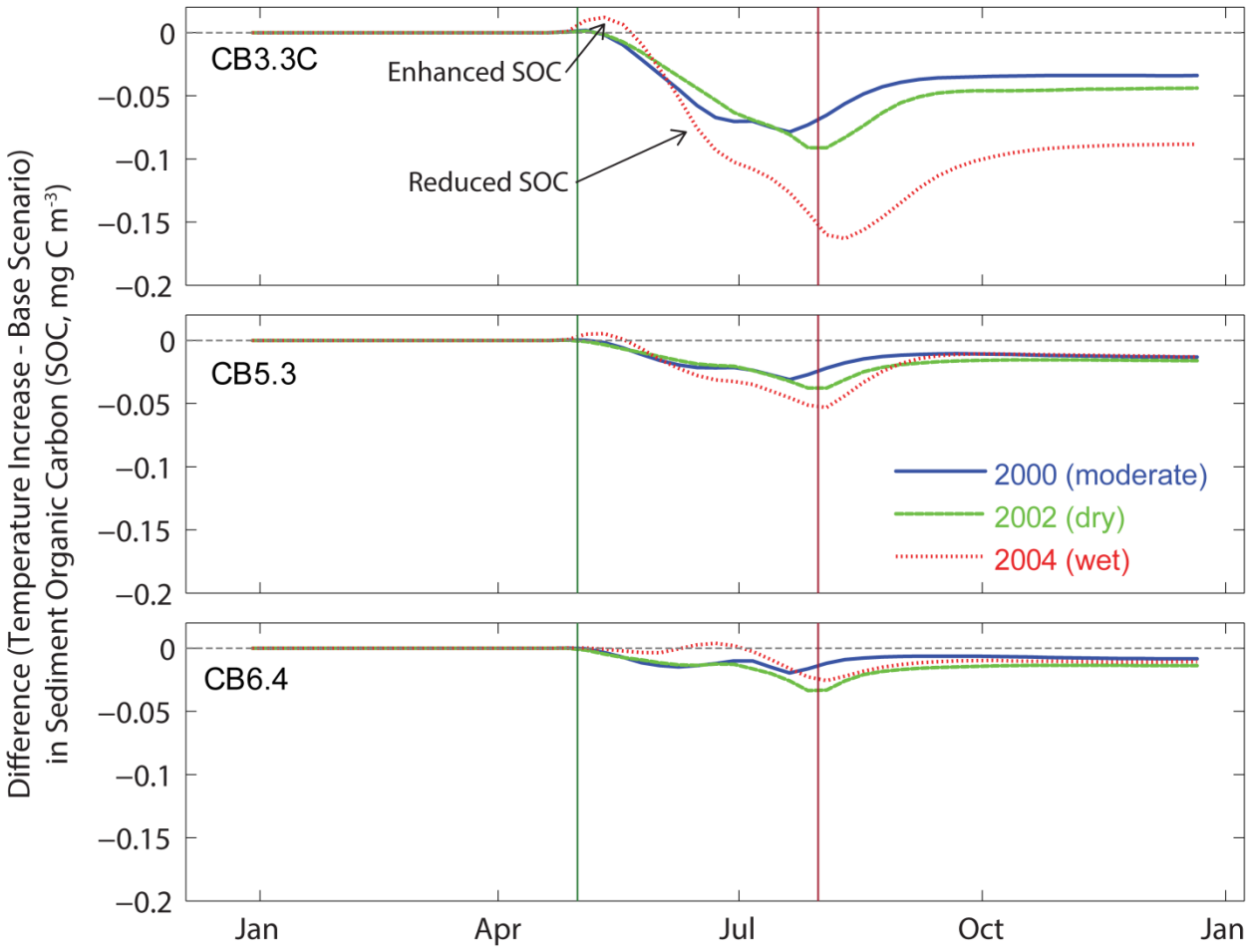

Figure 10: The difference in sediment organic carbon (SOC, mg C/m^3) between the seasonally-distinct temperature increase scenario and Base scenario at three locations in upper Bay (CB3.3C), the middle bay (CB5.3), and the lower Bay (CB6.4). The water temperature was increased Bay-wide by 1.5°C from May 1 (start, green line) to July 31 (stop, red line).

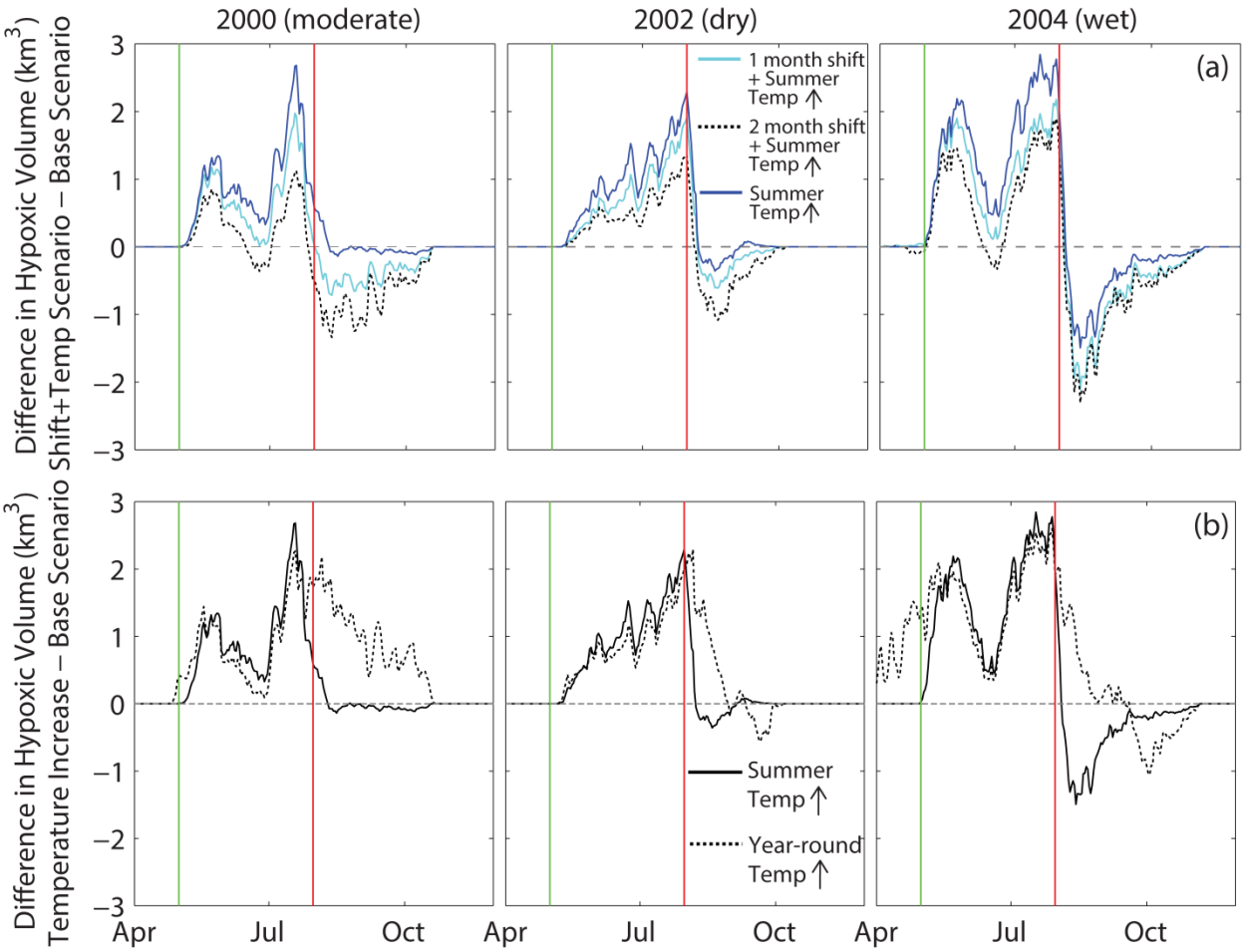

Figure 11: (a) Comparison of the hypoxic volumes resulting from combination scenarios of nutrient shift and water temperature increase in comparison to the Base scenario (no changes to nutrients or water temperature), at a hypoxia threshold of 2.0 mg O_2/L. The water temperature was increased Bay-wide by 1.5 °C from May 1 (start, green line) to July 31 (stop, red line), and the riverine NO_{23} was shifted 1 and 2 months early respectively. (b) Comparison of the hypoxic volumes resulting from the water temperature increase scenarios (seasonally-distinct, summer and year-round) in comparison to the Base scenario (no changes to nutrients or water temperature), at a hypoxia threshold of 2.0 mg O_2/L. For both scenarios the water temperature was increased Bay-wide by 1.5 °C. For the summer scenario this increase occurred from May 1 (start, green line) to July 31 (stop, red line), and for the year-round scenario, from January 1 to December 31.

Literature Cited

Ator, S. W., Blomquist, J. D., Webber, J. S., & Chanat, J. G. (2020). Factors driving nutrient trends in streams of the Chesapeake Bay watershed. *Journal of environmental quality, 49*(4), 812-834. doi: https://doi.org/10.1002/jeq2.20101

Bertani, I., Bhatt, G., Shenk, G. W., & Linker, L. C. (2021). Quantifying the Response of Nitrogen Speciation to Hydrology in the Chesapeake Bay Watershed Using a Multilevel Modeling Approach. *JAWRA Journal of the American Water Resources Association, n/a*(n/a). doi: https://doi.org/10.1111/1752-1688.12951

Boesch, D. F., Brinsfield, R. B., & Magnien, R. E. (2001). Chesapeake Bay eutrophication: Scientific understanding, ecosystem resotration, and challenges for agriculture. *Journal of Environmental Quality, 30*, 303-320.

Bouraoui, F., Grizzetti, B., Granlund, K., Rekolainen, S., & Bidoglio, G. (2004). Impact of Climate Change on the Water Cycle and Nutrient Losses in a Finnish Catchment. *Climatic Change, 66*(1), 109-126. doi: 10.1023/B:CLIM.0000043147.09365.e3

Boynton, W. R., & Kemp, W. M. (2008). Estuaries. In D. G. Capone, D. A. Bronk, M. R. Mulholland & E. J. Carpenter (Eds.), *Nitrogen in the marine environment* (2nd ed., pp. 809-866). Amsterdam: Elsevier.

Boynton, W. R., Kemp, W. M., & Keefe, C. W. (1982). A comparative analysis of nutrients and other factors influencing estuarine phytoplankton production. In V. S. Kennedy (Ed.), *Estuarine Comparisons* (pp. 69-90). New York.: Academic Press.

Brady, D. C., Targett, T. E., & Tuzzolino, D. M. (2009). Behavioral responses of juvenile weakfish (Cynoscion regalis) to diel-cycling hypoxia: swimming speed, angular correlation, expected displacement, and effects of hypoxia acclimation. *Canadian Journal of Fisheries and Aquatic Sciences, 66*(3), 415-424.

Brady, D. C., Testa, J. M., Di Toro, D. M., Boynton, W. R., & Kemp, W. M. (2013). Sediment flux modeling: calibration and application for coastal systems. *Estuarine, Coastal and Shelf Science 117*, 107-124.

Breitburg, D. L. (1994). Behavioral response of fish larvae to low dissolved oxygen concentrations in a stratified water column. *Marine Biology, 120*(4), 615-625.

Breitburg, D. L., Levin, L. A., Oschlies, A., Grégoire, M., Chavez, F. P., Conley, D. J., . . . Zhang, J. (2018). Declining oxygen in the global ocean and coastal waters. *Science, 359*(6371), eaam7240. doi: 10.1126/science.aam7240

Cai, X., Shen, J., Zhang, Y. J., Qin, Q., Wang, Z., & Wang, H. (2021). Impacts of sea-level rise on hypoxia and phytoplankton production in Chesapeake Bay: Model prediction and assessment. *JAWRA Journal of the American Water Resources Association, n/a*(n/a). doi: https://doi.org/10.1111/1752-1688.12921

Carstensen, J., Andersen, J. H., Gustafsson, B. G., & Conley, D. J. (2014). Deoxygenation of the Baltic Sea during the last century. *Proceedings of the National Academy of Sciences, 111*(15), 5628-5633. doi: 10.1073/pnas.1323156111

Chang, S. N., Wilusz, D. C., & Harman, C. J. (2018). *Effects of seasonal and long-term climate variability on nitrate export in the Chesterville Branch catchment of the Eastern Shore, MD.* Paper presented at the AGU Fall Meeting.

Chen, C.-C., Gong, G.-C., & Shiah, F.-K. (2007). Hypoxia in the East China Sea: One of the largest coastal low-oxygen areas in the world. *Marine Environmental Research, 64*, 399-408.

Cowan, J. L., & Boynton, W. R. (1996). Sediment-water oxygen and nutrient exchanges along the longitudinal axis of Chesapeake Bay: Seasonal patterns, controlling factors and ecological significance. *Estuaries, 19*, 562-580.

Díaz, R. J., & Rosenberg, R. (1995). Marine benthic hypoxia: A review of its ecological effects and the behavioural responses of benthic macrofauna. *Oceanography and Marine Biology: An Annual Review, 33*, 245-303.

Ding, H., & Elmore, A. J. (2015). Spatio-temporal patterns in water surface temperature from Landsat time series data in the Chesapeake Bay, USA. *Remote Sensing of Environment, 168*, 335-348.

Du, J., Shen, J., Park, K., Wang, Y.-P., & Yu, X. (2018). Worsened physical condition due to climate change contributes to the increasing hypoxia in Chesapeake Bay. *Science of The Total Environment, 630*, 707-717.

Elmore, A. J., Nelson, D. M., & Craine, J. M. (2016). Earlier springs are causing reduced nitrogen availability in North American eastern deciduous forests. *Nature Plants, 2*(10), 1–5.

Eshleman, K. N., Sabo, R. D., & Kline, K. M. (2013). Surface water quality is improving due to declining atmospheric N deposition. *Environmental Science & Technology, 47*(21), 12193-12200. doi: 10.1021/es4028748

Fisher, T. R., Fox, R. J., Gustafson, A. B., Koontz, E., Lepori-Bui, M., & Lewis, J. (2021). Localized Water Quality Improvement in the Choptank Estuary, a Tributary of Chesapeake Bay. *Estuaries and Coasts*. doi: 10.1007/s12237-020-00872-4

Frankel, L. T., Friedrichs, M. A. M., St-Laurent, P., Bever, A. J., Lipcius, R. N., Bhatt, G., & Shenk, G. W. (2022). Nitrogen reductions have decreased hypoxia in the Chesapeake Bay: Evidence from empirical and numerical modeling. *Science of The Total Environment, 814*, 152722. doi: https://doi.org/10.1016/j.scitotenv.2021.152722

Fulweiler, R. F., Nixon, S. W., Buckley, B. A., & Granger, S. L. (2007). Reversal of the net dinitrogen gas flux in coastal marine sediments. *Nature, 448*, 180-182

Greening, H., & Janicki, A. (2006). Toward reversal of eutrophic conditions in a subtropical estuary: Water quality and seagrass response to nitrogen loading reductions in Tampa Bay, Florida, USA. *Environmental management, 38*(2), 163-178.

Hagy, J. D., Boynton, W. R., Keefe, C. W., & Wood, K. V. (2004). Hypoxia in Chesapeake Bay, 1950-2001: Long-term change in relation to nutrient loading and river flow. *Estuaries, 27*, 634-658.

Hinson, K. E., Friedrichs, M. A. M., St-Laurent, P., Da, F., & Najjar, R. G. (2021). Extent and Causes of Chesapeake Bay Warming. *JAWRA Journal of the American Water Resources Association, n/a*(n/a). doi: https://doi.org/10.1111/1752-1688.12916

Irby, I. D., Friedrichs, M. A. M., Da, F., & Hinson, K. E. (2018). The competing impacts of climate change and nutrient reductions on dissolved oxygen in Chesapeake Bay. *Biogeosciences, 15*(9), 2649-2668. doi: 10.5194/bg-15-2649-2018

Jahan, R., & Choi, J. K. (2014). Climate Regime Shift and Phytoplankton Phenology in a Macrotidal Estuary: Long-Term Surveys in Gyeonggi Bay, Korea. [journal article]. *Estuaries and Coasts, 37*(5), 1169-1187. doi: 10.1007/s12237-013-9760-7

Kemp, W. M., Sampou, P. A., & Boynton, W. R. (1987). Relative roles of benthic versus pelagic oxygen-consuming processes in establishing and maintaining anoxia in Chesapeake Bay. In M. Mackiernan (Ed.), *Dissolved oxygen dynamics in Chesapeake Bay* (pp. 103-114): Maryland Sea Grant.

780 Kraus, R. T., Secor, D. H., & Wingate, R. L. (2015). Testing the thermal-niche oxygen-squeeze
781 hypothesis for estuarine striped bass. *Environmental Biology of Fishes, 98*(10), 2083-
782 2092. doi: 10.1007/s10641-015-0431-3
783 Kubo, A., Hashihama, F., Kanda, J., Horimoto-Miyazaki, N., & Ishimaru, T. (2019). Long-term
784 variability of nutrient and dissolved organic matter concentrations in Tokyo Bay between
785 1989 and 2015. *Limnology and Oceanography, 64*(S1), S209-S222. doi:
786 doi:10.1002/lno.10796
787 Lake, S. J., & Brush, M. J. (2015). Modeling estuarine response to load reductions in a warmer
788 climate: the York River Estuary, Virginia, USA. *Marine Ecology Progress Series 538*,
789 81-98.
790 Laurent, A., Fennel, K., Ko, D. S., & Lehrter, J. (2018). Climate change projected to exacerbate
791 impacts of coastal eutrophication in the northern Gulf of Mexico. *Journal of Geophysical*
792 *Research: Oceans, 123*(5), 3408-3426. doi: 10.1002/2017jc013583
793 Lee, M., Shevliakova, E., Malyshev, S., Milly, P. C. D., & Jaffé, P. R. (2016). Climate variability
794 and extremes, interacting with nitrogen storage, amplify eutrophication risk. *Geophysical*
795 *Research Letters, 43*(14), 7520-7528. doi: https://doi.org/10.1002/2016GL069254
796 Lee, Y. J., Boynton, W. R., Li, M., & Li, Y. (2013). Role of late winter-spring wind influencing
797 summer hypoxia in Chesapeake Bay. *Estuaries and Coasts, 36*(4), 683-696.
798 Lefcheck, J. S., Orth, R. J., Dennison, W. C., Wilcox, D. J., Murphy, R. R., Keisman, J., . . .
799 Batiuk, R. A. (2018). Long-term nutrient reductions lead to the unprecedented recovery
800 of a temperate coastal region. *Proceedings of the National Academy of Sciences, 115*(14),
801 3658-3662. doi: 10.1073/pnas.1715798115
802 Li, M., Lee, Y.-J., Testa, J. M., Li, Y., Ni, W., Kemp, W. M., & Toro, D. M. D. (2016). What
803 drives interannual variability of estuarine hypoxia: Climate forcing versus nutrient
804 loading? *Geophysical Research Letters, 43*(5), 2127-2134. doi: doi
805 10.1002/2015GL067334
806 Li, M., Zhong, L., & Boicourt, W. C. (2005). Simulations of Chesapeake Bay estuary: Sensitivity
807 to turbulence mixing parameterizations and comparison with observations. *Journal of*
808 *Geophysical Research, 110, C12004*. doi: doi:10.1029/2004JC002585
809 Li, M., Zhong, L., Boicourt, W. C., Zhang, S., & Zhang, D.-L. (2007). Hurricane-induced
810 destratification and restratification in a partially-mixed estuary. *Journal of Marine*
811 *Research 65*, 169-192.
812 Marshall, E., & Randhir, T. (2008). Effect of climate change on watershed system: a regional
813 analysis. *Climatic Change, 89*(3), 263-280. doi: 10.1007/s10584-007-9389-2
814 Meier, H. E. M., Andersson, H. C., Eilola, K., Gustafsson, B. G., Kuznetsov, I., Müller-Karulis,
815 B., . . . Savchuk, O. P. (2011). Hypoxia in future climates: A model ensemble study for
816 the Baltic Sea. *Geophysical Research Letters, 38*(24), L24608,
817 doi:24610.21029/22011GL049929.
818 Miller, W. D., & Harding, L. W. (2007). Climate forcing of the spring bloom in Chesapeake
819 Bay. *Marine Ecology Progress Series, 331*, 11-22.
820 Murphy, R. R., Kemp, W. M., & Ball, W. P. (2011). Long-term trends in Chesapeake Bay
821 seasonal hypoxia, stratification, and nutrient loading. *Estuaries and Coasts, 34*, 1293-
822 1309.
823 Ni, W., Li, M., Ross, A. C., & Najjar, R. G. (2019). Large projected decline in dissolved oxygen
824 in a eutrophic estuary due to climate change. *Journal of Geophysical Research: Oceans,*
825 *124*(11), 8271-8289. doi: 10.1029/2019jc015274

826 Ni, W., Li, M., & Testa, J. M. (2020). Discerning effects of warming, sea level rise and nutrient
827 management on long-term hypoxia trends in Chesapeake Bay. *Science of The Total*
828 *Environment, 737*, 139717. doi: https://doi.org/10.1016/j.scitotenv.2020.139717
829 Nixon, S. W., Fulweiler, R. W., Buckley, B. A., Granger, S. L., Nowicki, B. L., & Henry, K. M.
830 (2009). The impact of changing climate on phenology, productivity, and benthic-pelagic
831 coupling in Narragansett Bay. *Estuarine, Coastal and Shelf Science, 82*(1), 1-18.
832 Ortiz-Bobea, A., Wang, H., Carrillo, C. M., & Ault, T. R. (2019). Unpacking the climatic drivers
833 of US agricultural yields. *Environmental Research Letters, 14*(6), 064003. doi:
834 10.1088/1748-9326/ab1e75
835 Palinkas, C. M., Testa, J. M., Cornwell, J. C., Li, M., & Sanford, L. P. (2019). Influences of a
836 River Dam on Delivery and Fate of Sediments and Particulate Nutrients to the Adjacent
837 Estuary: Case Study of Conowingo Dam and Chesapeake Bay. *Estuaries and Coasts,*
838 *42*(8), 2072-2095. doi: 10.1007/s12237-019-00634-x
839 Riemann, B., Carstensen, J., Dahl, K., Fossing, H., Hansen, J. W., Jakobsen, H. H., . . .
840 Andersen, J. H. (2015). Recovery of Danish coastal ecosystems after reductions in
841 nutrient loading: A holistic ecosystem approach. [journal article]. *Estuaries and Coasts,*
842 *39*(1), 82-97. doi: 10.1007/s12237-015-9980-0
843 Sampou, P., & Kemp, W. M. (1994). Factors regulating plankton community respiration in
844 Chesapeake Bay. *Marine Ecology Progress Series, 110*, 249-258.
845 Savchuk, O. P. (2018). Large-Scale Nutrient Dynamics in the Baltic Sea, 1970–2016. [Original
846 Research]. *Frontiers in Marine Science, 5*(95). doi: 10.3389/fmars.2018.00095
847 Scavia, D., Justic, D., & V.J. Bierman, J. (2004). Reducing hypoxia in the Gulf of Mexico:
848 Advice from three models. *Estuaries and Coasts, 27*, 419-425.
849 Scavia, D., Kelly, E. L. A., & Hagy, J. D. (2006). A simple model for forecasting the effects of
850 nitrogen loads on Chesapeake Bay hypoxia. *Estuaries and Coasts, 29*, 674-684.
851 Shen, C., Testa, J. M., Ni, W., Cai, W.-J., Li, M., & Kemp, W. M. (2019). Ecosystem
852 Metabolism and Carbon Balance in Chesapeake Bay: A 30-Year Analysis Using a
853 Coupled Hydrodynamic-Biogeochemical Model. *Journal of Geophysical Research:*
854 *Oceans, 124*(8), 6141-6153. doi: https://doi.org/10.1029/2019JC015296
855 Stæhr, P. A., Testa, J. M., & Carstensen, J. (2017). Decadal changes in water quality and net
856 productivity of a shallow Danish estuary following significant nutrient reductions.
857 *Estuaries and Coasts, 40*, 63-79.
858 Taylor, D. I., Oviatt, C. A., Giblin, A. E., Tucker, J., Diaz, R. J., & Keay, K. (2020). Wastewater
859 input reductions reverse historic hypereutrophication of Boston Harbor, USA. *Ambio,*
860 *49*(1), 187-196. doi: 10.1007/s13280-019-01174-1
861 Testa, J. M., Basenback, N., C.Shen, Cole, K., Moore, A., Hodgkins, C., & Brady, D. C. (2021).
862 Modeling impacts of nutrient loading, warming, and boundary exchanges on hypoxia and
863 metabolism in a shallow estuarine ecosystem. *JAWRA Journal of the American Water*
864 *Resources Association, DOI :10.1111/1752-1688.12912*.
865 Testa, J. M., & Kemp, W. M. (2012). Hypoxia-induced shifts in nitrogen and phosphorus cycling
866 in Chesapeake Bay. *Limnology and Oceanography, 57*(3), 835-850.
867 Testa, J. M., & Kemp, W. M. (2014). Spatial and temporal patterns in winter-spring oxygen
868 depletion in Chesapeake Bay bottom waters. *Estuaries and Coasts, 37*(6), 1432-1448.
869 doi: doi: 10.1007/s12237-014-9775-8
870 Testa, J. M., Li, Y., Lee, Y. J., Li, M., Brady, D. C., Toro, D. M. D., & Kemp, W. M. (2014).
871 Quantifying the effects of nutrient loading on dissolved O_2 cycling and hypoxia in

Chesapeake Bay using a coupled hydrodynamic-biogeochemical model. *Journal of Marine Systems, 139*, 139-158. doi: doi:10.1016/j.jmarsys.2014.05.018

Testa, J. M., Murphy, R. R., Brady, D. C., & Kemp, W. M. (2018). Nutrient- and climate-induced shifts in the phenology of linked biogeochemical cycles in a temperate estuary. *Frontiers in Marine Science*, https://doi.org/10.3389/fmars.2018.00114.

Turner, R. E., Rabalais, N. N., & Justic, D. (2008). Gulf of Mexico hypoxia: Alternate states and a legacy. *Environmental Science and Technology, 42*(7), 2323-2327.

Verma, S., Bhattarai, R., Bosch, N. S., Cooke, R. C., Kalita, P. K., & Markus, M. (2015). Climate Change Impacts on Flow, Sediment and Nutrient Export in a Great Lakes Watershed Using SWAT. *CLEAN – Soil, Air, Water, 43*(11), 1464-1474. doi: https://doi.org/10.1002/clen.201400724

Wagena, M. B., Collick, A. S., Ross, A. C., Najjar, R. G., Rau, B., Sommerlot, A. R., . . . Easton, Z. M. (2018). Impact of climate change and climate anomalies on hydrologic and biogeochemical processes in an agricultural catchment of the Chesapeake Bay watershed, USA. *Science of The Total Environment, 637-638*, 1443-1454. doi: https://doi.org/10.1016/j.scitotenv.2018.05.116

Wang, B., Hu, J., Li, S., Yu, L., & Huang, J. (2018). Impacts of anthropogenic inputs on hypoxia and oxygen dynamics in the Pearl River estuary. *Biogeosciences, 15*(20), 6105-6125. doi: 10.5194/bg-15-6105-2018

Whitney, M. M., & Vlahos, P. (2021). Reducing hypoxia in an urban estuary despite climate warming. *Environmental Science & Technology, 55*(2), 941-951. doi: 10.1021/acs.est.0c03964

Yvon-Durocher, G., Jones, J. I., Trimmer, M., Woodward, G., & Montoya, J. M. (2010). Warming alters the metabolic balance of ecosystems. *Philosophical Transactions of the Royal Society B: Biological Sciences, 365*(1549), 2117-2126. doi: doi:10.1098/rstb.2010.0038

Zhang, Q., Brady, D. C., Boynton, W. R., & Ball, W. P. (2015). Long-term trends of nutrients and sediment from the nontidal Chesapeake watershed: An assessment of progress by river and season. *JAWRA Journal of the American Water Resources Association, 51*(6), 1534-1555.

Zhang, Q., Fisher, T. R., Trentacoste, E. M., Buchanan, C., Gustafson, A. B., Karrh, R., . . . Tango, P. J. (2021). Nutrient limitation of phytoplankton in Chesapeake Bay: Development of an empirical approach for water-quality management. *Water Research, 188*, 116407. doi: https://doi.org/10.1016/j.watres.2020.116407

Zhou, Y., Scavia, D., & Michalak, A. M. (2014). Nutrient loading and meteorological conditions explain interannual variability of hypoxia in Chesapeake Bay. *Limnology and Oceanography, 59*(2), 373-384.

List of Figures

Figure 1: (a) Chesapeake Bay ROMS-RCA model grid (water cells = red) and (b) Map of Chesapeake Bay's major tributaries and the Chesapeake Bay Program long-term water quality monitoring stations (CB3.3C, CB5.3, and CB6.4) that correspond to example locations for analysis in the upper, middle, and lower Bay, respectively.

Figure 2: Comparison of the daily total riverine flow (a) and cumulative daily riverine flow (b) of all major Chesapeake Bay tributaries (Susquehanna, Patuxent, Patapsco, Potomac, Choptank, Rappahannock, York, and James Rivers) to highlight that the years 2000 (moderate flow), 2002 (dry), and 2004 (wet) are hydrologically different.

Figure 3: (a) An example of the nutrient load timing shift scenarios for the seasonal concentration of nitrate and nitrite (NO_{23}) shifted to a peak one month early (dashed) and two months early (blue) for the Susquehanna River in 2000. This process was repeated for each hydrological year (2000, 2002, 2004) and tributary. (b) The resulting cumulative NO_{23} load of all tributaries combined, for each year and scenario.

Figure 4: Comparison of the difference between modeled mainstem Chesapeake Bay hypoxic volumes (<2 mg O_2/L) in the nutrient load (NO_{23}) shift scenarios and the baseline simulation (Nutrient Shift-Base) in each year 2000, 2002, and 2004.

Figure 5: Comparison of the difference in bottom layer dissolved oxygen (O_2) and total respiration respectively, between nutrient timing shift scenarios during the spring (January-May; a-c) and summer (June-August; d-f) seasons at three locations that represent the upper Bay (CB3.3C), the middle bay (CB5.3), and the lower Bay (CB6.4).

Figure 6: Model-simulated differences (Nutrient shift scenario-Base scenario) in sediment oxygen demand (SOD) for the one-month shift in NO_{23} concentration at three locations that represent the upper Bay (CB3.3C), the middle bay (CB5.3), and the lower Bay (CB6.4). Each of the three hydrologically unique years are included (2000, 2002, 2004).

Figure 7: Model-simulated differences (Nutrient shift scenario-Base scenario) in sediment water NH_4 flux (a) and sediment Particulate Organic Nitrogen concentration (PON, b) for the one-month shift in NO_{23} concentration at three locations that represent the upper Bay (CB3.3C), the middle bay (CB5.3), and the lower Bay (CB6.4). Each of the three hydrologically unique years are included (200, 2002, 2004).

Figure 8: Seasonal difference (warming-Base) in modeled mainstem hypoxia (<2.0 mg O_2/L) in each of three hydrologic years in response to idealized, seasonally-distinct water temperature increase (warming) scenario, where water temperature was increased Bay-wide by 1.5 °C from May 1 (start, green line) to July 31 (stop, red line).

Figure 9: The difference in (a) sediment oxygen demand (SOD) and (b) total respiration between the seasonally-distinct temperature increase scenario and the Base scenario in the upper Bay (CB3.3C), the middle bay (CB5.3), and the lower Bay (CB6.4). The water temperature was increased Bay-wide by 1.5°C from May 1 (start, green line) to July 31 (stop, red line).

Figure 10: The difference in sediment organic carbon (SOC, mg C/m^3) between the seasonally-distinct temperature increase scenario and Base scenario at three locations in upper Bay (CB3.3C), the middle bay (CB5.3), and the lower Bay (CB6.4). The water temperature was increased Bay-wide by 1.5°C from May 1 (start, green line) to July 31 (stop, red line).

Figure 11: (a) Comparison of the hypoxic volumes resulting from combination scenarios of nutrient shift and water temperature increase in comparison to the Base scenario (no changes to nutrients or water temperature), at a hypoxia threshold of 2.0 mg O_2/L. The water temperature was increased Bay-wide by 1.5 °C from May 1 (start, green line) to July 31 (stop, red line), and the riverine NO_{23} was shifted 1 and 2 months early respectively. (b) Comparison of the hypoxic volumes resulting from the water temperature increase scenarios (seasonally-distinct, summer and year-round) in comparison to the Base scenario (no changes to nutrients or water temperature), at a hypoxia threshold of 2.0 mg O_2/L. For both scenarios the water temperature was increased Bay-wide by 1.5 °C. For the summer scenario this increase occurred from May 1 (start, green line) to July 31 (stop, red line), and for the year-round scenario, from January 1 to December 31.